K- and L-shell ionization of atoms by relativistic electrons

James H. Scofield
Lawrence Livermore Laboratory, University of California, Livermore, California 94550
(Received 5 June 1978)

Results of a relativistic calculation of the cross section for the ionization from the K and L shells by high-energy electrons are presented. The calculations use the first-order Born approximation to treat the interaction between the scattered and atomic electrons. Plane waves are used to treat the high-energy scattered electron, while solutions of the Dirac equation in a Hartree-Slater central potential are used to describe the atomic electrons. Results are presented for a set of elements from $Z = 18$ to 92 and incident energies from 50 keV to 1 GeV. Calculated results are given for the correction due to the density effect arising from the polarizability of the medium. In the calculation of this correction, the medium is treated as composed of free electons.

I. INTRODUCTION

In this paper the cross sections for the ionization of electrons from the K and L shells are calculated. The calculation uses the relativistic form of the first-order Born approximation with plane waves used to treat the high-energy electron. The atomic and ejected electrons are treated as moving in the Hartree-Slater central potential. To calculate the total cross section, the differential cross section for the scattering with a particular energy loss and scattering angle is integrated over.

Relativistic calculations of the ionization cross sections have previously been carried out using nonrelativistically derived values of the matrix elements based either on the Coulomb potential[1,2] or on the connection with the cross section for photoionization.[3] A completely relativistic calculation attempted by Perlman[4] for a Coulomb potential contains numerical errors.

For small momentum transfers, the differential cross section is approximately proportional to the photoionization cross section. This proportionality leads to a simple form for the energy dependence of the total cross section in the high-energy limit. This form of the energy dependence was introduced in the work of Bethe.[5] We present fits to the calculated cross sections with this form as the asymtotic limit.

An important effect entering the stopping power at high energies is the density effect[6] due to the polarizability of the medium. The effect leads to a saturation of the energy-loss cross section at high energies. We have carried out a calculation of the effect in the subshell ionization cross sections by treating the modifying electrons as free. It has been pointed out by Dangerfield[7] that the effect seems to be absent in the experimental results for the subshell ionization cross sections. Further investigations of the effect are needed.

II. THEORY

We distinguish between the high-energy electron and the electron ejected from the atom. This is feasible for bombarding energies much greater than the binding energies since, in general, the energy loss to the ejected electron is of the order of the binding energy; and thus, interference effects between the scattered and ejected electron will be small. The high-energy electron is described by plane-wave solutions of the Dirac equation. The atomic electrons are treated relativistically as moving in a central potential. The first-order Born approximation is used to treat the interaction of the high-energy and atomic electrons. The differential cross section for the scattering of an electron with initial four momentum p_μ and final momentum p'_μ with the excitation of the atomic system from state a to b is given by

$$\frac{d\sigma}{d\Omega p'} = \left(\frac{2e^2 p'}{pq^4}\right) \sum_{\mu\nu} \left(p_\mu p'_\nu + p'_\mu p_\nu + \frac{g_{\mu\nu} q^2}{2} \right) J^\mu J^{\nu *} , \tag{1}$$

with $J^\mu = e\langle \bar{\psi}_b e^{i\vec{k}\cdot\vec{r}} \gamma^\mu \psi_a \rangle$, in units such that $\hbar = c = m = 1$, where m is the electron's rest mass. We denote by ϵ and ϵ' the scattered electron's initial and final total relativistic energy. We use $W = \epsilon - \epsilon'$ to denote the energy transferred; $\vec{k} = \vec{p} - \vec{p}'$ the three momentum transfer; and q^2 the square of the four-momentum transfer $q^2 = k^2 - W^2$. The longitudinal and timelike components of the current are related by charge conservation, therefore,

$$\vec{k} \cdot \vec{J} = W J^0 . \tag{2}$$

For the atomic wave functions we use solutions of the Dirac equation in a central potential with[9]

$$\psi_{jlm} = \frac{i^l}{r} \begin{pmatrix} G(r)\chi_\kappa(\hat{r}) \\ iF(r)\chi_{-\kappa}(\hat{r}) \end{pmatrix} ; \tag{3}$$

$$\chi_\kappa(\hat{r}) = \sum_{m,\mu} C(l\tfrac{1}{2}j; m_l \mu) Y_{l m l}(\hat{r}) \zeta_\mu . \tag{4}$$

In terms of κ, the total and orbital angular momentum are given by

$$j = |\kappa| - \tfrac{1}{2}$$

and

$$l = |\kappa + \tfrac{1}{2}| - \tfrac{1}{2} . \tag{5}$$

The standard representation of the γ matrices have been assumed and ζ are two component spinors. The bound-state wave functions are normalized by

$$\int (G^2 + F^2)\, dr = 0 , \tag{6}$$

and the amplitude of the contunuum states are fixed by

$$\lim_{r\to\infty} [G^2 + F^2]_{av} = \tfrac{1}{2} . \tag{7}$$

The matrix elements are calculated by using the vector multipole expansion[10] instead of the plane-wave form of the exchanged radiation field

$$\begin{aligned}
\vec{A}^{(m)}_{LM}(\vec{k},\vec{r}) &= i^L [L(L+1)]^{-1/2} j_L(kr) \vec{L} Y_{LM}(\hat{r}) , \\
\vec{A}^{(e)}_{LM}(\vec{k},\vec{r}) &= i^L [L(L+1)]^{-1/2} k^{-1} \vec{\nabla} \times \vec{L} j_L(kr) Y_{LM}(\hat{r}) , \\
\vec{A}^{(l)}_{LM}(\vec{k},\vec{r}) &= i^{L-1} k^{-1} \vec{\nabla} j_L(kr) Y_{LM}(\hat{r}) .
\end{aligned} \tag{8}$$

Directional measurements are assumed not made on the ejected electron or on the atomic states so averages are taken over the magnetic quantum numbers of the initial states and sums over those of the final.

The differential cross section is given by

$$\begin{aligned}
d\sigma &= (4\alpha^2 N_a\, dq^2 dW)/(\beta_b p^2) \\
&\times \{2(\epsilon\epsilon' - \tfrac{1}{4}q^2) T_l(k^2, W)/(k^2 W^2) \\
&+ [\tfrac{1}{2} - 1/q^2 + (\epsilon\epsilon' - \tfrac{1}{4}q^2)/k^2] T_\perp(k^2, W)/q^2 \} ,
\end{aligned} \tag{9}$$

with

$$\begin{aligned}
T_l(k^2, W) &= (2j_b + 1)\, X(\kappa_a, \kappa_b, L) R^2_l (2L+1) , \\
T_\perp &= T_e + T_m , \\
T_e(k^2, W) &= (2j_b+1) X(\kappa_a, \kappa_b, L) R^2_e (2L+1)/L(L+1) , \\
T_m(k^2, W) &= (2j_b+1) X(-\kappa_a, \kappa_b, L) R^2_m (2L+1)/L(L+1) ,
\end{aligned} \tag{10}$$

with N_a denoting number of electrons in the subshell and β_b the velocity of the ejected electron. The angular momentum factors X are given in terms of the three-j and six-j symbols as

$$X(\kappa_a, \kappa_b, L) = (2l_a+1)(2l_b+1) \begin{pmatrix} l_a & l_b & L \\ 0 & 0 & 0 \end{pmatrix}^2 \begin{Bmatrix} L & l_a & l_b \\ \frac{1}{2} & j_b & j_a \end{Bmatrix}^2 . \tag{11}$$

For a given κ_a of the initial subshell, the sums over L and κ_b range over all values for which the angular factors are not zero. For the factors to be nonzero the final state must have the correct parity and its angular momentum is restricted by the triangle condition. In a numerical calculation the matrix elements become sufficiently small for large values of L that the sum over L can be terminated and a given accuracy maintained. The radial matrix elements are

$$\begin{aligned}
R_l &= \int dr \Big(-(G_b F_a - F_b G_a) j_{(L-1)}(kr) \\
&\quad + [(\kappa_b - \kappa_a)(G_b F_a + F_b G_a) \\
&\quad + (L+1)(G_b F_a - F_b G_a)] \frac{j_L(kr)}{(kr)} \Big) , \\
R_e &= \int \left(\frac{dr}{kr}\right) \Big[(F_b G_a - G_b F_a) L(L+1) j_L(kr) \\
&\quad + (\kappa_b - \kappa_a)(F_b G_a + G_b F_a) \left(r\frac{d}{dr} + 1 \right) j_L(kr) \Big] , \\
R_m &= (\kappa_a + \kappa_b) \int dr (F_b G_a + G_b F_a) j_L(kr) .
\end{aligned} \tag{12}$$

The subscripts $\perp$, e, m, and l refer to the transverse, electric, magnetic, and longitudinal components, respectively.

The total ionization cross section is given by integrating over the range of q^2 corresponding to different scattering angles and over the range of possible energy transfers. For a given energy loss, q^2 ranges from

$$q^2_{\min} = [W/(p+p')]^2 [(\epsilon+\epsilon')^2 + (p+p')^2]/(\epsilon\epsilon' + pp') \tag{13a}$$

to

$$q^2_{\max} = 2(\epsilon\epsilon' - 1 + pp') . \tag{13b}$$

The range for the energy transfer is from $W_{\min} = E_a$, E_a the subshell binding energy, to $W_{\max} = \epsilon - 1$. If the energy of the ejected electron is much greater than the binding energy, the cross section, integrated over the scattering angle, will be the same as for the scattering from a free electron, that is,

$$d\sigma = \pi\alpha^2 N_a dW [\epsilon^2 + \epsilon'^2 - 2(\epsilon - \epsilon')]/p^2 W^2 , \tag{14}$$

in the case, as here, in which we distinguish between the scattered and ejected electron. The transverse components enter the photoionization cross section

$$\sigma_{\rm ph}(W) = (4\pi\alpha N_a/W\beta_b) T_\perp(W^2, W) . \tag{15}$$

For small values of the momentum transfer the matrix elements are independent of direction and thus $T_l = \frac{1}{2} T_\perp$.

For large values of the incident energy, the variation in the cross section comes from the variation of the lower limit of the integration. The matrix elements can be taken as constant near the lower

TABLE I. K-shell ionization cross sections in barns for various elements and incident electron kinetic energies.

MeV/Z	18	28	39	47	56	67	79	83	92
0.05	1970	524.5	158.5						
0.10	1283	367.8	131.2	67.6	32.32				
0.15	1026	301.8	112.6	61.0	31.97	14.61			
0.20	895	266.7	101.7	56.5	30.70	15.07	6.77	5.07	
0.30	764	231.9	90.7	51.6	29.07	15.19	7.56	5.95	3.38
0.40	704	215.9	85.7	49.4	28.41	15.30	7.98	6.41	3.86
0.50	672	207.7	83.4	48.5	28.25	15.52	8.32	6.76	4.20
0.60	654	203.4	82.3	48.3	28.36	15.81	8.64	7.08	4.49
0.80	638	200.4	82.1	48.6	28.94	16.45	9.24	7.64	4.97
1.00	636	200.9	83.0	49.5	29.72	17.11	9.78	8.14	5.39
2.00	666	214.2	90.3	54.8	33.59	19.93	11.85	10.02	6.90
5.00	760	248.2	106.5	65.5	40.88	24.84	15.23	13.03	9.24
10.00	848	279.7	121.1	74.9	47.12	28.94	17.98	15.46	11.10
20.00	943	313.0	136.3	84.8	53.58	33.14	20.76	17.91	12.96
50.00	1072	358.2	157.0	98.0	62.22	38.70	24.43	21.12	15.38
100.00	1171	392.7	172.7	108.1	68.7	42.91	27.18	23.53	17.19
200.00	1270	427.4	188.4	118.1	75.32	47.11	29.92	25.93	18.99
500.00	1401	473.2	209.3	131.5	83.97	52.65	33.53	29.08	21.35
1000.00	1501	508.0	225.1	141.5	90.51	56.83	36.25	31.47	23.13

limit and the total cross section has a simple form coming from the explicit q^2 dependence near this limit. For ϵ large

$$\sigma = (A/\beta^2)(\ln p^2 - \beta^2 - b)\,, \tag{16}$$

where β is the velocity of the incident electron. For A we have

$$A = \left(\frac{\alpha}{\pi}\right)\int_{E_a}^{\infty} \frac{dW\sigma_{\rm ph}}{W}\,. \tag{17}$$

TABLE II. $L1$-subshell ionization cross sections in barns.

MeV/Z	18	28	39	47	56	67	79	83	92
0.05	24 349	6627	2347	1284	691.6	361.3	184.4	147.4	84.9
0.10	14 900	4128	1495	833	460.8	252.6	139.0	115.0	73.6
0.15	11 598	3241	1185	665	371.5	206.7	116.0	96.8	63.5
0.20	9932	2791	1026	578	325.0	182.3	103.4	86.6	57.5
0.30	8291	2347	870	493	279.0	158.0	90.7	76.2	51.2
0.40	7514	2138	797	453	257.6	146.8	84.8	71.5	48.4
0.50	7086	2025	757	432	246.4	141.0	81.9	69.2	47.0
0.60	6830	1958	735	420	240.2	137.9	80.4	68.0	46.4
0.80	6569	1893	714	409	235.0	135.6	79.5	67.3	46.1
1.00	6466	1871	708	407	234.4	135.7	79.9	67.7	46.6
2.00	6547	1917	734	424	246.1	143.8	85.4	72.6	50.3
5.00	7179	2132	826	481	280.8	165.3	98.9	84.2	58.6
10.00	7826	2346	915	535	313.4	185.3	111.2	94.7	66.0
20.00	8528	2575	1011	592	348.1	206.4	124.2	105.7	73.8
50.00	9486	2889	1141	671	395.3	235.0	141.6	120.6	84.2
100.00	10 220	3129	1240	730	431.3	256.9	155.0	132.0	92.2
200.00	10 958	3370	1340	791	467.5	278.8	168.3	143.3	100.1
500.00	11 934	3689	1473	870	515.3	307.8	186.0	158.3	110.6
1000.00	12 674	3931	1573	930	551.5	329.7	199.3	169.7	118.5

TABLE III. $L2$-subshell ionization cross sections in barns.

MeV/Z	18	28	39	47	56	67	79	83	92
0.05	51 601	11 133	3429	1793	938.5	479.9	234.6	182.5	100.2
0.10	32 166	7045	2204	1172	631.2	339.7	181.9	148.0	92.4
0.15	25 214	5574	1755	939	510.2	279.1	153.3	126.2	81.5
0.20	21 713	4824	1525	819	447.1	246.8	137.4	113.7	74.6
0.30	18 267	4085	1298	700	384.6	214.5	121.3	101.0	67.4
0.40	16 647	3740	1192	645	355.7	199.7	114.0	95.2	64.2
0.50	15 765	3555	1136	616	340.5	192.0	110.4	92.5	62.8
0.60	15 250	3448	1104	600	332.1	188.0	108.6	91.2	62.2
0.80	14 752	3351	1076	586	325.4	185.2	107.8	90.7	62.4
1.00	14 589	3325	1070	583	324.8	185.5	108.6	91.6	63.3
2.00	14 984	3450	1116	611	342.0	197.2	116.9	99.1	69.5
5.00	16 725	3896	1267	697	391.5	227.6	136.6	116.3	82.5
10.00	18 444	4328	1411	778	438.0	255.8	154.4	131.7	94.0
20.00	20 296	4792	1566	864	487.5	285.6	173.1	148.0	106.0
50.00	22 825	5423	1777	982	554.7	326.0	198.5	169.9	122.2
100.00	24 761	5907	1938	1072	606.2	356.9	217.8	186.6	134.5
200.00	26 705	6392	2100	1163	657.7	387.9	237.2	203.3	146.9
500.00	29 281	7036	2314	1283	726.0	428.8	262.8	225.5	163.2
1000.00	31 232	7523	2476	1373	777.7	459.9	282.2	242.2	175.5

III. CALCULATED RESULTS

To describe the atomic electrons, we use the relativistic version of the Hartree-Slater central potential model. We have used the same version of the model for the calculation of x-ray emission rates[10] and of photoionization cross sections.[11] The calculated values of the energy eigenvalues are used as the binding energies.

The calculated values of the ionization cross sections are given in Tables I–IV for the ionization from the K and L subshells. Calculated results

TABLE IV. $L3$-subshell ionization cross sections in barns.

MeV/Z	18	28	39	47	56	67	79	83	92
0.05	104 520	22 965	7227	3866	2090	1141	623.0	510.6	326.6
0.10	65 038	14 521	4635	2515	1392	790	461.0	388.3	268.3
0.15	51 053	11 484	3686	2010	1121	644	381.9	324.0	228.4
0.20	43 960	9937	3199	1750	979	566	338.8	288.4	205.2
0.30	36 977	8412	2720	1493	839	489	295.3	252.3	181.2
0.40	33 695	7699	2496	1373	774	453	275.2	235.6	170.1
0.50	31 908	7316	2376	1310	739	434	264.8	227.1	164.5
0.60	30 863	7096	2308	1274	720	423	259.3	222.6	161.7
0.80	29 853	6894	2248	1242	704	415	255.4	219.6	160.1
1.00	29 521	6840	2234	1236	701	415	255.8	220.1	160.9
2.00	30 314	7094	2327	1292	735	437	271.6	234.3	172.3
5.00	33 830	8007	2638	1468	837	500	312.6	270.2	199.6
10.00	37 303	8892	2936	1637	934	559	350.5	303.1	224.4
20.00	41 046	9842	3256	1817	1037	622	390.5	337.9	250.5
50.00	46 154	11 138	3691	2062	1177	707	444.7	385.0	285.6
100.00	50 066	12 130	4024	2249	1284	773	486.0	420.8	312.4
200.00	53 994	13 125	4359	2437	1392	838	527.5	456.8	339.2
500.00	59 199	14 445	4802	2687	1534	924	582.3	504.4	374.7
1000.00	63 140	15 443	5137	2875	1642	990	623.8	540.4	401.6

TABLE V. K-shell theoretical electron binding energies and parameters fitting ionization cross section and density correction (see text).

Z	E_a(keV)	A (barn)	B_1	B_2	B_3	B_4	B_5	C_1	C_2	ξ
18	3.178	71.77	6.7542	-0.218	-0.0123	0.0129	-0.0008	0.5474	1.1375	0.8943
28	8.303	25.06	6.1081	-0.494	-0.0457	0.0087	-0.0035	0.5506	1.1339	0.8958
39	17.001	11.39	5.6060	-0.863	-0.1118	-0.0240	-0.0103	0.5594	1.1493	0.8921
47	25.49	7.271	5.3083	-1.164	-0.1721	-0.0670	-0.0199	0.5577	1.1479	0.8916
56	37.45	4.719	5.0231	-1.539	-0.2383	-0.1331	-0.0388	0.5576	1.1528	0.8890
67	55.71	3.017	4.6810	-2.021	-0.2887	-0.2356	-0.0787	0.5545	1.1594	0.8847
79	81.00	1.963	4.3119	-2.545	-0.2977	-0.3876	-0.1482	0.5495	1.1751	0.8756
83	90.90	1.716	4.1875	-2.704	-0.3010	-0.4553	-0.1763	0.5373	1.1647	0.8795
92	116.28	1.280	3.9104	-2.990	-0.3729	-0.6650	-0.2389	0.5282	1.1816	0.8684

TABLE VI. $L1$-subshell binding energies and fitting parameters.

Z	E_a(keV)	A (barn)	B_1	B_2	B_3	B_4	B_5	C_1	C_2	ξ
18	0.3134	534.0	9.5745	-0.045	0.0029	0.0070	-0.0001	0.4134	1.2588	0.8140
28	1.006	174.5	8.3637	-0.109	0.0020	0.0122	-0.0003	0.4407	1.2347	0.8307
39	2.355	72.39	7.5703	-0.211	-0.0065	0.0142	-0.0007	0.4619	1.2322	0.8369
47	3.783	43.51	7.2272	-0.306	-0.0186	0.0124	-0.0012	0.4684	1.2267	0.8402
56	5.961	26.16	6.9270	-0.448	-0.0377	0.0078	-0.0022	0.4748	1.2252	0.8430
67	9.362	15.84	6.6504	-0.647	-0.0646	-0.0024	-0.0048	0.4781	1.2234	0.8441
79	14.34	9.644	6.5112	-0.930	-0.1064	-0.0244	-0.0099	0.4783	1.2203	0.8460
83	16.39	8.201	6.5334	-1.042	-0.1294	-0.0377	-0.0118	0.4841	1.2327	0.8424
92	21.80	5.721	6.5568	-1.318	-0.2254	-0.0910	-0.0139	0.4841	1.2351	0.8412

TABLE VII. $L2$-subshell binding energies and fitting parameters.

Z	E_a(keV)	A (barn)	B_1	B_2	B_3	B_4	B_5	C_1	C_2	ξ
18	0.2494	1408.	8.0191	-0.022	0.0031	0.0047	-0.0001	0.4891	1.1030	0.8941
28	0.8850	351.7	7.2318	-0.067	0.0024	0.0091	-0.0001	0.5422	1.1034	0.9036
39	2.160	117.2	6.9703	-0.160	-0.0056	0.0133	-0.0004	0.5504	1.1172	0.9043
47	3.528	65.53	6.8021	-0.254	-0.0139	0.0171	-0.0010	0.5549	1.1164	0.9050
56	5.630	37.34	6.6686	-0.400	-0.0230	0.0247	-0.0025	0.5589	1.1204	0.9043
67	8.929	22.41	6.3612	-0.593	-0.0348	0.0311	-0.0056	0.5574	1.1231	0.9025
79	13.778	14.01	5.9793	-0.826	-0.0702	0.0158	-0.0093	0.5543	1.1325	0.8981
83	15.77	12.11	5.8539	-0.908	-0.0924	0.0019	-0.0103	0.5524	1.1357	0.8967
92	21.05	8.912	5.5370	-1.091	-0.1604	-0.0416	-0.0108	0.5469	1.1442	0.8913

TABLE VIII. $L3$-subshell binding energies and fitting parameters.

Z	E_a(keV)	A (barn)	B_1	B_2	B_3	B_4	B_5	C_1	C_2	ξ
18	0.2471	2845.	8.0338	-0.018	0.0003	0.0019	0	0.4880	1.1002	0.8952
28	0.8670	721.1	7.2579	-0.056	-0.0032	0.0034	0	0.5435	1.1004	0.9050
39	2.0814	242.2	7.0524	-0.136	-0.0142	0.0044	-0.0002	0.5540	1.1146	0.9063
47	3.350	136.2	6.9504	-0.217	-0.0254	0.0056	-0.0008	0.5605	1.1135	0.9072
56	5.243	77.89	6.9275	-0.345	-0.0406	0.0087	-0.0023	0.5655	1.1131	0.9087
67	8.061	47.25	6.7878	-0.514	-0.0601	0.0112	-0.0051	0.5672	1.1121	0.8183
79	11.92	29.98	6.6509	-0.724	-0.0985	0.0017	-0.0089	0.5678	1.1136	0.9087
83	13.42	26.00	6.6242	-0.800	-0.1201	-0.0067	-0.0100	0.5680	1.1150	0.9086
92	17.18	19.38	6.5610	-0.973	-0.1899	-0.0362	-0.0112	0.5659	1.1132	0.9083

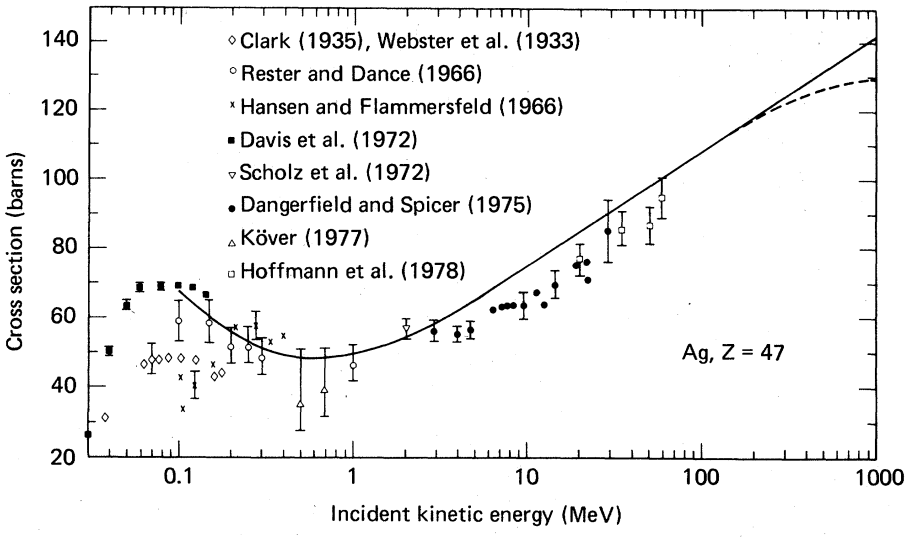

FIG. 1. K-shell ionization cross section for silver as a function of incident energy. Solid curve is present calculation without density effect. Dashed curve includes the density effect for normal solid silver. The sources for the experimental points are given in Ref. 13. Representative error bars are from the reports of the experimental measurements.

are presented for a number of elements from $Z=18$ to $Z=92$ and for those energies between 50 keV to 1 GeV which are greater than twice the given subshell's binding energy. The numerical accuracy is of the order of 0.1%.

In Tables V–VIII are given the calculated binding energies and the parameters giving a fit as a function of the incident energy. The form of the fit for the cross section given in barns is

$$\sigma=(A/\beta^2)(B+b_1+b_2/\epsilon+b_3/p^2+b_4B/p+b_5/p^4)\,, \tag{18}$$

with

$$B=\ln(p^2)-\beta^2\,.$$

In terms of the incident kinetic energy $\epsilon=1+\epsilon_k/mc^2$, $p^2=\epsilon^2-1$, and $\beta=p/\epsilon$.

The effect of the polarization is included treating the electrons of the medium as free, by replacing the propagator for the transverse photon $1/q^2$ by $1/(q^2+\omega_p^2)$. The plasma frequency ω_p is given by

$$\omega_p^2=4\pi e^2NZ/m\,, \tag{19}$$

with N the atomic density. This cutoff of the singularity of the transverse propagator is the major effect of the density effect in the high-energy limit. The matrix elements can be approximated by their values with the momentum transfer that of a real photon. The correction to the cross section thus reads

$$\delta=\left(\frac{\alpha}{\pi\beta^2}\right)\int\left(\frac{dW}{W}\right)\sigma_{\rm ph}(W)\left\{\left[1+\left(\frac{\omega_p p}{W}\right)^2\right]+\frac{\beta^2}{\left[(W/\omega_p p)^2+1\right]}\right\}. \tag{20}$$

In the region with β close to one, the correction is function of the combination $\omega_p p$ for a given element and subshell. In Tables V–VIII the results of the calculation of the density effect are given by giving the parameters for a fit to the results. The form of the fit is

$$\delta=A\{-(1/\xi)\ln[1+(C_\omega p^2)^\xi]+C_2/[1+(C_\omega p^2)^{-\xi}]\}\,, \tag{21}$$

with

$$C_\omega=C_1(\omega_p/E_a)^2\,.$$

Here β has been assumed equal to one and the calculations were carried out at solid densities. The saturation value of the cross section is given by

$$\sigma_\infty=A[-\ln(C_\omega)+b_1-1+C_2]\,. \tag{22}$$

Figure 1 shows the calculated and the experimental values for the ionization from the K shell of silver ($Z=47$) and Fig. 2 shows those for gold ($Z=79$). The sources for the experimental values are given in Ref. 13. In the case of silver the calculated value including the effect of the density effect for 10.5 g/cm^3 are shown. At this density $\omega_p=61.4$ eV and the cross section saturates at a value of 132 b.

IV. DISCUSSION

By using wavefunctions for a Hartree-type potential and the relativistic calculation of the matrix elements, the present calculation is an advancement over previous relativistic calculations. A number of areas remain for future studies.

The atomic model used here gives results for the photoionization cross section which agree in general with experimental measurements to within 5% in the K- and L-shell ionization region.[14]

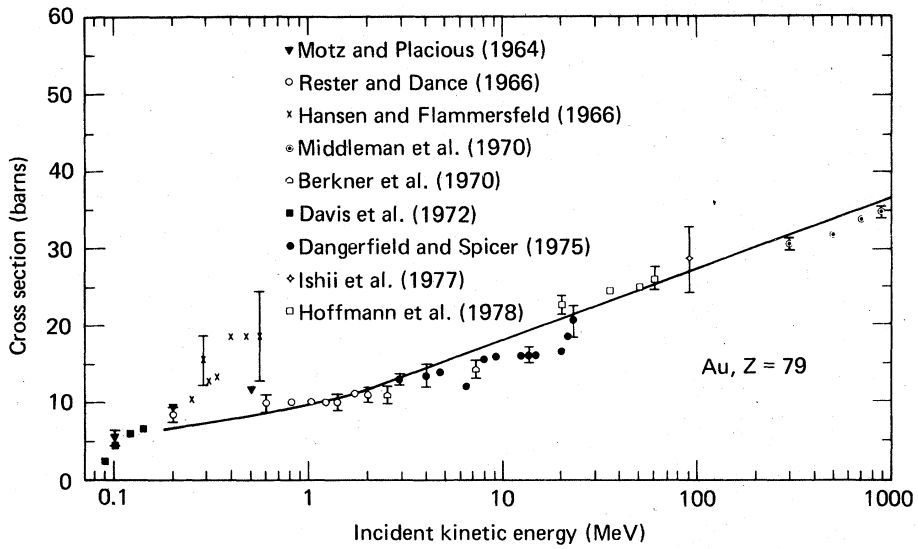

FIG. 2. K-shell ionization cross section for gold as a function of incident electron energy. Solid curve is present calculation. The sources for the experimental points are given in Ref. 13.

The inaccuracies in the wavefunctions should not introduce substantially larger errors into the calculation of the gross features of the electron ionization cross sections. As emphasized by Madison,[15] the differential cross sections, which have been integrated over in the present calculation, will be more demanding of the model used for the electron ionization cross section.

For electron energies no longer large compared with the electron's binding energy, the neglect of exchange and the use of the Born approximation with plane waves are no longer valid. A formulation which should be valid for substantially lower energies in the case of inner shell ionization from high Z elements is to solve for the wavefunctions of the scattered electron as well as the atomic electrons in the potential and to take the exchange into account. Such a calculation would be interesting but formidable for relativistic electrons.

An interesting puzzle remains as to why the data of Middleman *et al.*[13] does not show the saturation due to the density effect for the lower Z elements. An explanation might lie in taking into account the excitation of the medium or of the distribution of momentum transfers accompaning the scattering of an electron within the nuclear potential. In any case further experimental and theoretical studies will be of interest.

ACKNOWLEDGMENTS

The author wishes to thank H. Genz, H. Tawara, K. Ishii, and B. M. Spicer for information on their experimental results. This work was supported by the U.S. Department of Energy by the Lawrence Livermore Laboratory under contract No. W-7405-ENG-48.

[1]A. M. Arthurs and B. L. Moiseiwitsch, Proc. Soc. Lond. A 247, 550 (1958).
[2]D. M. Davidović and B. L. Moiseiwitsch, J. Phys. B 8, 947 (1975).
[3]H. Kolbenstvedt, J. Appl. Phys. 38, 4785 (1967).
[4]H. S. Perlman, Proc. Phys. Soc. Lond. A 76, 623 (1960).
[5]H. A. Bethe, Ann. Phys. 5, 325 (1930); *Handbuch der Physik*, edited by H. Geiger and K. Scheel (Springer, Berlin, 1933), Vol. 24/1 p. 273. Recent discussions are given by U. Fano, Phys. Rev. 95, 1198 (1954); M. Inokuti, Rev. Mod. Phys. 43, 297 (1971); C. A. Quarles, Phys. Lett. A 39, 375 (1972).
[6]See the discussion by U. Fano, Ann. Rev. Nucl. Sci. 13, 1 (1963); R. M. Sternheimer, in *Methods of Experimental Physics*, edited by L. C. L. Yuan and C.-S. Wu (Academic, New York, 1961), Vol. 5, Part A, p. 1; A. Crispin and G. N. Fowler, Ref. 8.
[7]G. R. Dangerfield, Phys. Lett. A 46, 19 (1973); see also the discussion by H. Tawara, in *Electronic and Atomic Collisions*, edited by G. Watel (North-Holland, Amsterdam, 1978), p. 311.
[8]A. Crispin and G. N. Fowler, Rev. Mod. Phys. 42, 290 (1970).
[9]See M. E. Rose, *Relativistic Electron Theory* (Wiley, New York, 1961).
[10]See, for example, J. H. Scofield in *Atomic Inner-Shell Ionization*, (Academic, New York, 1975), p. 265.
[11]J. H. Scofield, Phys. Rev. 179, 9 (1969).
[12]J. H. Scofield, Lawrence Livermore Laboratory Report UCRL-51326 (1973); available from National Technical Information Center, National Bureau of Standards, Springfield, Virginia 22151.
[13]J. C. Clark, Phys. Rev. 48, 30 (1935); D. L. Webster,

W. W. Hansen, and F. B. Duveneck, *ibid.* 43, 839 (1933); J. W. Motz and R. C. Placious, *ibid.* 136, A 662 (1964); D. H. Rester and W. E. Dance, *ibid.* 152, 1 (1966); H. Hansen and A. Flammersfeld, Nucl. Phys. 79, 135 (1966); L. M. Middleman, R. L. Ford, and R. Hofstadter, Phys. Rev. A 2, 1429 (1970); K. H. Berkner, S. N. Kaplan, and R. V. Pyle, Bull. Am. Phys. Soc. 15, 786 (1970); D. V. Davis, V. D. Mistry, and C. A. Quarles, Phys. Lett. A 38, 169 (1972); W. Scholz, A. Li-Scholz, R. Collé, and I. L. Preiss, Phys. Rev. Lett. 29, 761 (1972): G. R. Dangerfield and B. M. Spicer, J. Phys. B 8, 1744 (1975); K. Ishii, M. Kamiya, K. Sera, S. Morita, H. Tawara, M. Oyamad, and T. C. Chu, Phys. Rev. A 15, 906 (1977); Á. Kövér, Nucl. Instrum. 142, 5 (1977); D. H. H. Hoffmann, H. Genz, W. Löw and A. Richter, Phys. Lett. A 65, 304 (1978).

[14]J. H. Hubbell and W. J. Veigle, *Comparison of Theoretical and Experimental Photoeffect Data 0.1 keV to 1.5 MeV*, National Bureau of Standards, Technical Note 901 (U. S. GPO, Washington, D. C., 1976).

[15]D. H. Madison, *Proceedings of the Second International Conference Innershell Ionization Phenomena* (University of Freiburg, Freiburg, 1976), Part I, p. 321.